Talanta 98 (2012) 277–281

Contents lists available at SciVerse ScienceDirect

Talanta

journal homepage: www.elsevier.com/locate/talanta

Short communication

Novel hybrid organic–inorganic monolithic column containing mesoporous nanoparticles for capillary electrochromatography

Li Wan [a], Lingyi Zhang [a], Wen Lei [a], Yaxian Zhu [a], Weibing Zhang [a,*], Yanqin Wang [b,**]

[a] Shanghai Key Laboratory of Functional Materials Chemistry, East China University of Science and Technology, Shanghai 200237, PR China
[b] Lab for Advanced Materials, Research Institute of Industrial Catalysis, East China University of Science and Technology, Shanghai 200237, PR China

ARTICLE INFO

Article history:
Received 23 March 2012
Received in revised form
27 June 2012
Accepted 1 July 2012
Available online 13 July 2012

Keywords:
CEC
Incorporating
Mixed mode
SBA-15 mesoporous nanoparticles
Hybrid organic–inorganic monolithic column

ABSTRACT

The rod-shaped SBA–15–C_{18} mesoporous nanoparticles were incorporated into hybrid organic–inorganic monolithic column with aminopropyl moiety to develop novel stationary phases with mixing mechanism of reverse phase and ion exchange. Experimental conditions including dispersion pattern, nanoparticles percentage were optimized for simple and stable column preparation. The monolithic columns were evaluated with mixture of organic acids in capillary electrochromatography (CEC) mode and the column efficiency reaches 280, 000 plates/m. The results indicate that the column containing nanoparticles enhances both selectivity and column efficiency due to high specific surface area of nanoparticles and mixing separation mechanism.

1. Introduction

Nanoparticles possess a large surface-to-volume ratio as well as multiform morphologies, which potentially facilitate mass transfer and improve column efficiency and selectivity chromatography separation [1–3]. Although the small particle size of nanoparticles is good for fast mass transfer and high column efficiency, ultra high pressure during column packing and separation process has been a challenge. For example, column packed with 1.7 μm particle can achieve ultra column efficiency but requires over 137.9 Mpa pressure for running. Consequently, nanoparticles could not be easily applied into chromatography in form of conventional packing column, even in capillary electrochromatography (CEC) [4], in which electric drive force instead of high pressure is employed. The applications of nanomaterials in CEC mostly focus on pseudostationary phase (PSP)–CEC [5] and open-tubular CEC [6,7]. However, these applications were restricted by low phase ratio of open-tubular column and disturbance of detection caused by light-scattering of nanoparticles in PSP-CEC.

Monolithic stationary phase, which has been developed rapidly in recent years, promotes the applications of nanomaterials in CEC. Hydroxyapatite nanoparticles [8], single-wall carbon nanotubes (SWNT) [9] and multiwalled carbon nanotubes [10] were respectively incorporated into organic polymer monolith for separation of small molecules, proteins and peptides. Bonn et al. [11] prepared monolithic extraction columns based on poly(divinylbenzene) with TiO_2 and ZrO_2 nano-powders embedded for selective enrichment of phosphorylated peptides. Weichelt et al. [12] have prepared porous monolithic inorganic/polymeric hybrid materials for applications in tissue engineering, which were via ring-opening metathesis copolymerization in the presence of inorganic nanoparticles. Hybrid particle-monolithic polymethacrylate columns [13] were prepared by in situ polymerization in capillaries pre-packed with particles for micro-HPLC. In addition, nanoparticles can be attached to the pore surface of preformed monoliths via simple electrostatic binding or in situ reaction. For example, Hilder et al. [14] have attached quaternary amine-functionalized latex particles to sulfonic acid functionalized monolith via electrostatic interaction. Haddad's group [15–19] applied this method for the preparation of columns for ion chromatography and CEC. Also, Krenkova prepared a new monolithic column with iron oxide nanoparticles coating recently [20]. Frechet et al. [21,22] have attached gold nanoparticles via in situ reduction of chloroauric acid to pore surface of monolith within the column. Zhang et al. [23] developed a novel Ti^{4+}–IMAC (immobilized metal affinity chromatography) by sol–gel method

Abbreviations: id, inside diameter; od, outside diameter; RSD, relative standard deviation; PSP, pseudostationary phase; SWNT, single-wall carbon nanotubes; TEOS, tetraethoxysilane; APTES, 3-aminopropyltriethoxysilane

* Corresponding author. Tel.: +86 021 64252145; fax: +86 021 64233161.
** Corresponding author. Tel.: +86 21 64253824; fax: +86 21 64253703.
E-mail addresses: weibingzhang@ecust.edu.cn (W. Zhang), wangyanqin@ecust.edu.cn (Y. Wang).

0039-9140/$ - see front matter © 2012 Elsevier B.V. All rights reserved.
http://dx.doi.org/10.1016/j.talanta.2012.07.002

and Ti^{4+} chelate immobilization for the analysis of mitochondrial phosphoproteome. Connolly [24] used photografting methods to improve the homogeneity of gold nanoparticles attached on surface of polymer monolith for the first time and proved that nanoparticles increased the effective surface area of the polymer monolith significantly.

In most of the work mentioned above, organic polymer monolith was taken as matrix due to easy preparation with good control of porosity, wide pH range and high reproducibility. However, shortcomings of shrinking and swelling of organic polymer monolith in different solvents lead to negative effects on pore structure and mechanical properties of organic polymer monolith [25]. As an attractive alternative, hybrid organic–inorganic monoliths combine the advantages of silica with organic polymer monolithic material, such as good biocompatibility, high mechanical strength, and favorable solvent resistance property [26–29]. It has been successfully used as the separation matrix of chromatographic column [30,31] and immobilized enzyme [32,33] reactor. Yan et al. [34,35] developed a series organic–inorganic hybrid porous silica-based monolithic stationary phases for CEC separation. By using 3-aminopropyl triethoxysilane (APTES) as one of precursors, organic aminopropyl moiety was introduced into silica bones and resultant hybrid matrix was fabricated without drying procedure to avoid shrinkage or crack of gel [31,36]. Besides, the SBA-15 silica material with highly ordered mesoporous structure is of significant value to chromatographic separation owing to its unique properties of high surface areas, extremely narrow pore size distribution, perfectly adjustable pore size, and the presence of silanol groups [37,38]. Hyphenation of hybrid organic–inorganic monolith and nanoparticles would combine advantages of two materials and improve chromatographic performance significantly.

Spherical-particle has been usually widely used because its easy-packing, high efficiency, good stability and low backpressure compared with irregular-particle. However, when considering embedment of nanoparticles into monolith, particle shape would not be a key factor. In this study, a novel organic–inorganic hybrid monolithic stationary phase containing rod-shape SBA–15–C_{18} nanoparticles was developed by one step copolymerization and applied for CEC with mixed-mode mechanism. Nanoparticles cannot be moved by applying pressure or electric drive force. Prepared columns were evaluated by separating of five organic acids mixture and ethanol extract of *gastrodia elata Bl.* to explore its retention mechanism.

2. Materials and methods

2.1. Materials and chemicals

All CEC experiments were carried out using a Trisep 2003 GHV002 CEC system (Unimicro Shanghai Technologies Co., Ltd., USA) consisting of a UV-absorbance detector. Data acquisition and processing were done using software of Trisep 2003 chromatography data handing system. A Vortex mixer was used for mixing samples and sol solutions (QL-901, Kylin-Bell Lab Instruments Co., Ltd. China). Ultrasonic cleaner was used for dispersing nanoparticles and removing bubbles (AS3120, Tianjin Aote Saiensi Instrument Co., Ltd. China). The cross section of the monolithic column was examined by scanning electron microscopy (SEM) system (JSM-6360LV, Japan). Surface area was obtained by adsorption–desorption isotherms of liquid nitrogen (ASAP2010N, America). Fused-silica capillaries of 75 μm i.d. and 375 μm o.d. were purchased from Sino Sumtech (Hebei, China).

The rod-shaped SBA–15–C_{18} [39] mesoporous silicon materials were provided by group of Prof. Yanqin Wang. Tetraethoxysilane (98%) and 3-aminopropyltriethoxysilane (99%) were purchased from Acros (Shanghai, China), which were used directly without further purification. Cetyltrimethyl ammonium bromide was purchased from Crystal pure reagent (Shanghai, China).

2.2. Preparation of hybrid organic–inorganic monolithic column with SBA-15 nanoparticles

Fused silica capillary was pretreated before in situ copolymerization as described elsewhere [31]. A mixture containing 3.6 mg CTAB, 56 μL TEOS, 59 μL APTES, 110 μL ethanol, 13 μL water and varying quantities of nanoparticles was ultrasonicated for 1 min after vibrating for 2 min at 0 °C to get a homogeneous suspension. It was then filled into the pretreated capillary with syringe. The capillary columns were sealed with rubber and reacted at room temperature for 12 h. The column was then washed with ethanol and water respectively to remove CTAB and other residual of reactants. The total length and effective length of the column (named as TEOS–APTES–SBA–15 column in following statement) were 21 cm and 11 cm respectively. Hybrid monolithic column without nanoparticles (named as TEOS–APTES column) was prepared as control column using sol–gel methods described elsewhere [31].

2.3. Preparation of ethanol extract of gastrodia elata Bl.

8 g of *gastrodia elata Bl.* added into 60% ethanol in 80 mL solution was heated to 70 °C for 4 h, which was repeated 3 times. The cooled solution was filtered through Büchner funnel filtration and 0.45 μm filter membrane respectively.

3. Results and discussion

3.1. Effect of nanoparticles dispersion

The dispersion of nanoparticles in monolithic matrix can affect pore structure, separation efficiency and repeatability. Therefore, it is necessary to evenly distribute nanoparticles in reaction mixture to form uniform stationary phase in capillary. Two methods were used to disperse SBA-15 particles: mixing with vortex mixer only and mixing with vortex mixer and ultrasonic cleaner in order. Although the reaction solution became gel after 5 min at room temperature and no sediment of nanoparticles was observed after 10 min when using reaction solution without catalyst (see Fig. S-1), the vortex mixing still resulted in column clogging. By performing vortex mixing and ultrasonic mixing in order, the column shows good performance (see Table S-1) and stability with relative standard deviation (RSD) of retention times less than 5% ($n=7$). It was considered that sediment of nanoparticles didn't damage their uniform distribution in hybrid organic–inorganic monolith by using vortex and ultrasonic mixing in order.

3.2. Effect of nanoparticles percentage

Different percentages of nanoparticles in reaction mixture, 10, 16 and 28 mg/mL, were used to prepare hybrid columns to investigate their effects on retention behavior of columns by separating five organic acids. Increasing of nanoparticles percentage leads to embedding of more nanoparticles in the pore of monolithic matrix which provides higher specific area.

By the co-condensation of TEOS and APTES, the surface of prepared monolithic column is positively charged, which results in the direction of EOF from cathode to anode. When using 10 mg/mL suspension for preparation, the EOF was $3.1\times10^{-7}\,m^2v^{-1}s^{-1}$. Almost the same EOF ($2.5\times10^{-7}$ and $2.4\times10^{-7}\,m^2v^{-1}s^{-1}$) was observed using 16 mg/mL and 28 mg/mL nanoparticles

suspension, which indicates that incorporation of nanoparticles decreases the density of amino groups and reduces reversed EOF.

Fig. 1 (A, B) shows better separation performance using 16 mg/mL nanoparticle suspension than the 10 mg/mL one. The capacity factor (k*) are enhanced by increasing nanoparticles percentage (see Table S-2). However, when the percentage was increased to 28 mg/mL (C), o-aminobenzoic acid and phthalic acid cannot be separated due to aggregation of high percentage nanoparticles. Aggregation also resulted in poor permeability and preparation repeatability. Besides, the permeabilities of hybrid monolithic columns with different percentage nanoparticles were examined (see Table S-3). The results indicate that the back pressures are increased by increasing the percentage of nanoparticles.

From above, 16 mg/mL was chosen in following experiments.

3.3. Characterization of nanoparticles and column

The SEM analysis confirmed rod-shape SBA-15 nanoparticles with an average size of 1.5 μm in length and 300–400 nm in width (Fig. 2C). The SEM images clearly shows morphology change of monolith after incorporation of nanoparticles. The TEOS–APTES–SBA-15 column (B) has uniform porous structure and smaller flow-through pores. The BET surface area of monolith containing nanoparticles (62.98 m^2/g) is significantly increased comparing to monolith without nanoparticles (38.17 m^2/g).

3.4. Exploration separation mechanism

3.4.1. Separation of neutral compounds

To confirm the RP separation ability of SBA-15-C_{18} particles, a neutral test mixture containing thiourea, o-xylene and naphthalene was eluted according to their hydrophobicity (Fig. 3 A), which demonstrates that the nanoparticles were successfully incorporated

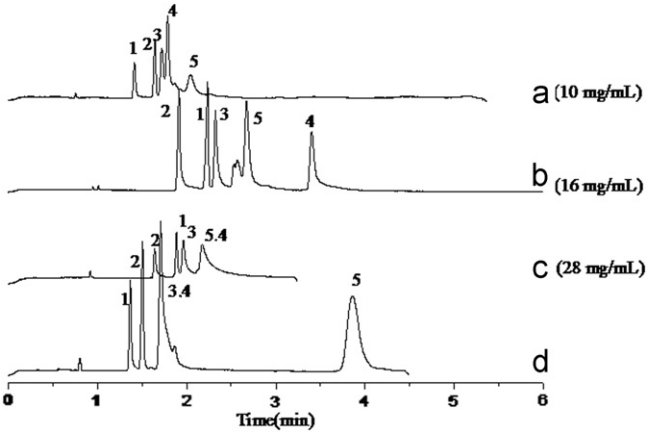

Fig. 1. The separation of organic acids; Columns: (A) (B) (C) TEOS–APTES–SBA-15 columns with 10 mg/mL, 16 mg/mL, and 28 mg/mL SBA-15 rods (D) TEOS–APTES; Experimental conditions: mobile phase, 25 mM NaH_2PO_4 (pH=4.35) containing 50% acetonitrile; Applied voltage, −8 kv; Temperature, 25 °C; UV–vis detector wave length, 214 nm. Sample: (1) sulfanilic acid (pKa=3.32), (2) salicylic acid (pKa=2.98), (3) o-iodobenzoic acid (pKa=2.85), (4) phthalic acid (pKa=2.95), (5) o-aminobenzoic acid (pKa=4.98) * unknown impurity.

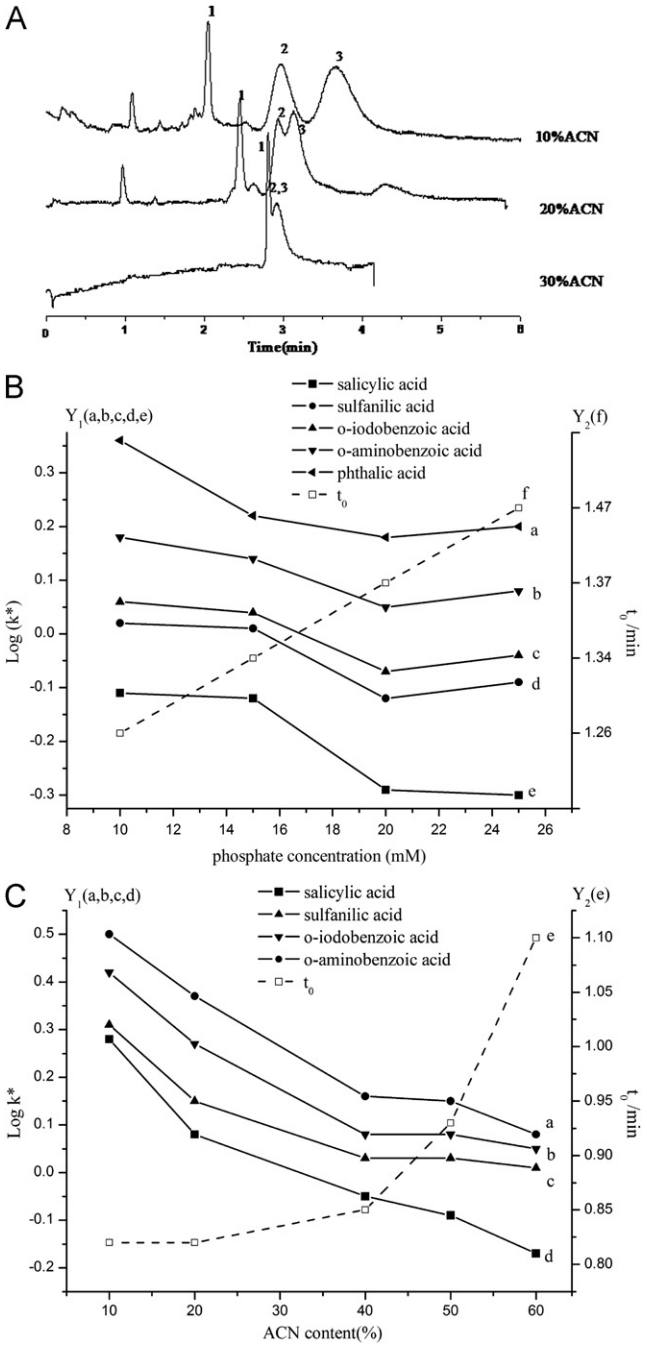

Fig. 3. Effect of mobile phase composition on separation of neutral compounds and retention factors (k*) of organic acids.; (A) effect of organic modifier on separation of neutral compounds; effect of ion strength (B) and organic modifier content (C) on k* of organic acids.; Columns: TEOS–APTES–SBA-15. Experimental conditions: mobile phase, (A) 25 mM NaH_2PO_4 (pH=2.45) containing 10%, 20%, 30% acetonitrile, respectively; (B) NaH_2PO_4 (pH=4.35) containing 50% acetonitrile with buffer concentrations ranging from 10 to 25 mM; (C) 25 mM NaH_2PO_4 (pH=4.35) containing 10%, 20%, 40%, 50% and 60% acetonitrile, respectively; Samples: (A) (1) thiourea (2) o-xylene (3) naphthalene; samples in (B,C) are the same as in Fig. 1.

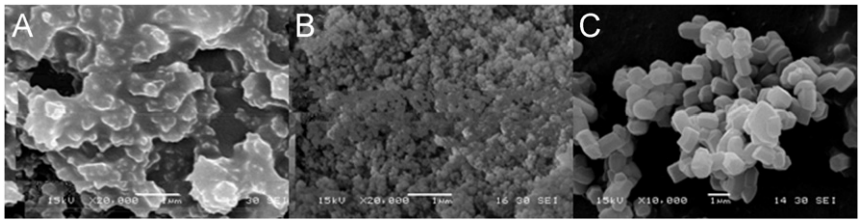

Fig. 2. SEM images of TEOS–APTES column (A), TEOS–APTES–SBA-15 column (B) at 20,000x magnification and SBA-15 nanoparticles (C) at 10,000x.

into the TEOS–APTES–SBA-15 column. But the column efficiency is low because only small amount of SBA-15-C_{18} particles was incorporated into monolith.

The effect of the acetonitrile content in the range from 10 to 30% (v/v) on the separation was studied while keeping the ionic strength constant in the mobile phase. It was observed that the electro osmotic mobility decreased about 27% when the acetonitrile content increased from 10 to 30%. It is because that the increase of acetonitrile content decreases the electro osmotic mobility by decreasing the ratio of the dielectric constant and the viscosity (ε/η) and the ζ-potential of the surface of the monolithic material. The resolutions and k* of thiourea, o-xylene and naphthalene are decreased significantly by adding more acetonitrile in mobile phase (see Fig. S-2), which follows the RP separation mechanism.

3.4.2. Separation of organic acids

To further explore the separation mechanism, the five organic acids were separated using hybrid TEOS–APTES–SBA-15 column (B) and TEOS–APTES column (D) as shown in Fig. 1. Five organic acids are only successfully separated on the column b. Both retention and separation efficiency are enhanced by incorporation of SBA-15 particles (see Table S-4). The column efficiency of sulfanilic acid reaches 280, 000 plates/m.

From Fig. 1, different elution order were found when using TEOS–APTES column, TEOS–APTES–SBA-15 columns prepared with different percentage of SBA-15-C_{18} particles. TEOS–APTES column developed by Yan etc. [31] has positively charged surface and suits for the separation of negatively charged analytes in WAX–CEC mode. The direction of EOF is from cathode to anode. The separation mechanism of charged compounds on this column is the combination of electrophoretic mobility and anion exchange interaction, although the relative contributions of them to the retention behavior of the acidic compounds are opposite. At pH 4.35, o-aminobenzoic acid is positive charged and its electrophoresis migration direction is against direction of EOF. Then, although there is no anion exchange interaction between o-aminobenzoic acid and amino group of TEOS–APTES column, o-aminobenzoic acid was eluted as the last one (Fig. 1 D). When adding 10 mg/mL SBA-15-C_{18} particles, the elution order is as same as that of TEOS–APTES column. By increasing amount of nanoparticles, the elution orders of salicylic acid and sulfanilic acid, phthalic acid and o-aminobenzoic acid are reversed due to hydrophobic interaction, which indicates incorporation of nanoparticles modified by hydrophobic groups change separation mechanism gradually. Because the SBA-15 mesoporous nanoparticles functionalized by trimethoxyoctadecylsilane provide reversed phase groups, the separation mechanism of containing SBA-15-C_{18} nanoparticles has been changed to mixing mechanism of weak anion exchange, electrophoresis, and reversed phase mechanisms.

3.4.3. Effect of ionic strength and organic modifier content on separation of organic acids

The influence of ionic strength on the separation was investigated at various phosphate buffer concentrations from 10 to 25 mM in the mobile phase containing 50% (v/v) acetonitrile while keeping pH at 4.35 (Fig. 3 B). As the ionic strength of mobile phase increased, the electrostatic interactions were reduced and the retention of negative charged compounds decreased. On the other hand, the decrease of electrophoretic mobility of acidic compound results in an increase of k* value. Variation of ionic strength has no effect on hydrophobic interaction. Then, similar to results of Yan etc. [31], the retention factors tend to decrease slightly with the increase of ionic strength, which indicates both electrokinetic migration and anion exchange interaction contribute to retention of acidic compounds, and the latter one plays predominant role under these conditions.

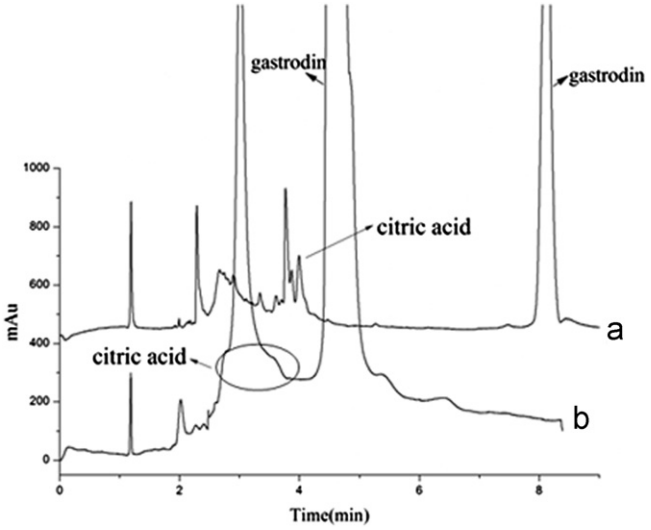

Fig. 4. The separation of ethanol extract of Gastrodia elata Bl.; Columns: (A) TEOS–APTES–SBA-15 (B) TEOS–APTES; Experimental conditions: mobile phase, 20 mM NaH_2PO_4 (pH = 5.0) containing 20% acetonitrile; other conditions are the same as in Fig. 1.

Acetonitrile content in the range from 10 to 60% (v/v) were also investigated too (Fig. 3C). Similar to separation of neutral compounds, EOF was decreased. The electrochromatographic retention factors show reducing trend with the increase of acetonitrile content in the mobile phase, which suggested that the interaction between the organic acids and mixing mode stationary phase (functionalized by both C_{18} and amino groups) weakened. Comparing to TEOS–APTES column, acetonitrile content has greater effect on retention of organic acids because content of organic modifier result in not only reducing of dielectric constants but also strengthening of hydrophobicity of mobile phase.

3.5. Repeatability

Injection-to-injection and batch-to-batch repeatability were investigated under the optimized preparation condition. The RSD values of retention time are less than 2.5% (see Table S-5) for five consecutive runs, which shows good stability of monolithic column with nanoparticles incorporated. Batch-to-batch repeatability was calculated by testing 3 columns, which were prepared at the same condition. The RSD values less than 10% owes to simple and stable preparation procedure.

3.6. Application

Gastrodia elata Bl. is a perennial herb, which is used for the treatment of headache, dizziness, limb numbness and other diseases. As a natural product, it has complicated chemical composition and contains active ingredients gastrodin. From Fig. 4 (A, B), compared with TEOS–APTES column, there are more peaks separated by TEOS–APTES–SBA-15 column, which demonstrated that the new column possesses different separation selectivity. By comparing with retention time of reference substance, gastrodin and citric acid were identified and separated by TEOS–APTES–SBA-15 column.

4. Concluding remarks

Based on advantage of hybrid organic–inorganic material and nanomaterial, a novel hybrid organic–inorganic monolithic columns

containing rod-shape nanoparticles with mixing mechanism has been developed. The TEOS–APTES–SBA-15 column described here is a potentially powerful tool for separation of complex samples in view of its mixing separation mechanism and good column efficiency. By changing functional monomers and using nanoparticles with multiple chemical modifications, this preparation method facilitates an easy tailoring of the interactions between sample and stationary phase. This investigation will expand the application of nanomaterial in chromatography.

Acknowledgment

We gratefully acknowledge the support of the Fundamental Research Funds for the Central Universities of China (WK1014042), the National Science Foundation for Young Scientists of China (no.21105027), and the Science and Technology Commission of Shanghai Municipality (no. 10dz2220500).

Appendix A. Supporting information

Supplementary data associated with this article can be found in the online version at http://dx.doi.org/10.1016/j.talanta.2012.07.002.

References

[1] E. Guihen, J.D. Glennon, Anal. Lett. 36 (2003) 3309–3336.
[2] C. Nilsson, S. Birnbaum, S. Nilsson, J. Chromatotogr. A 1168 (2007) 212–224.
[3] C. Nilsson, S. Nilsson, Electrophoresis 27 (2006) 76–83.
[4] R. Tian, J. Sun, H. Zhang, M. Ye, C. Xie, J. Dong, J. Hu, D. Ma, X. Bao, H. Zou, Electrophoresis 27 (2006) 742–748.
[5] C. Nilsson, P. Viberg, P. Spégel, M. Jörntén-Karlsson, P. Petersson, S. Nilsson, Anal. Chem. 78 (2006) 6088–6095.
[6] Y.L. Hsieh, T.H. Chen, C.Y. Liu, Electrophoresis 27 (2006) 4288–4294.
[7] Q. Qu, D. Liu, D. Mangelings, C. Yang, X. Hu, J. Chromatotogr. A 1217 (2010) 6588–6594.
[8] J. Krenkova, N.A. Lacher, F. Svec, Anal. Chem. 82 (2010) 8335–8341.
[9] Y. Li, Y. Chen, R. Xiang, D. Ciuparu, L.D. Pfefferle, C. Horwath, J.A. Wilkins, Anal. Chem. 77 (2005) 1398–1406.
[10] S.D. Chambers, F. Svec, J.M.J. Frechet, J. Chromatogr. A 1218 (2011) 2546–2552.
[11] M. Rainer, H. Sonderegger, R. Bakry, C.W. Huck, S. Morandell, L.A. Huber, D.T. Gjerde, G.K. Bonn, Proteomics 8 (2008) 4593–4602.
[12] F. Weichelt, S. Lenz, S. Tiede, I. Reinhardt, B. Frerich, M.R. Buchmeiser, Beilstein J. Org. Chem. 6 (2010) 1199–1205.
[13] C. Hou, J. Ma, D. Tao, Y. Shan, Z. Liang, L. Zhang, Y. Zhang, J. Proteome Res. 9 (2010) 4093–4101.
[14] E.F. Hilder, F. Svec, J.M.J. Frechet, J. Chromatogr. A 1053 (2004) 101–106.
[15] J.P. Hutchinson, E.F. Hilder, M. Macka, N. Avdalovic, P.R. Haddad, J. Chromatogr. A 1109 (2006) 10–18.
[16] J.P. Hutchinson, E.F. Hilder, R.A. Shellie, J.A. Smith, P.R. Haddad, Analyst 131 (2006) 215–221.
[17] J.P. Hutchinson, M. Macka, N. Avdalovic, P.R. Haddad, J. Chromatogr. A 1106 (2006) 43–51.
[18] J.P. Hutchinson, P. Zakaria, A.R. Bowiet, M. Macka, N. Avdalovic, P.R. Haddad, Anal. Chem. 77 (2005) 407–416.
[19] P. Zakaria, J.P. Hutchinson, N. Avdalovic, Y. Liu, P.R. Haddad, Anal. Chem. 77 (2005) 417–423.
[20] J. Krenkova, F. Foret, J. Sep. Sci. 34 (2011) 2106–2112.
[21] Q. Cao, Y. Xu, F. Liu, F. Svec, J.M.J. Frechet, Anal. Chem. 82 (2010) 7416–7421.
[22] Y. Xu, Q. Cao, F. Svec, J.M.J. Frechet, Anal. Chem. 82 (2010) 3352–3358.
[23] P. Jandera, J. Urban, V. Škeříková, P. Langmaier, R. Kubíčková, J. Planeta, J. Chromatogr. A 1217 (2010) 22–33.
[24] D. Connolly, B. Twamley, B. Paull, Chem. Commun. 46 (2010) 2109–2111.
[25] H.F. Zou, X.D. Huang, M.L. Ye, Q.Z. Luo, J. Chromatogr. A 954 (2002) 5–32.
[26] W. Li, D.P. Fries, A. Malik, J. Chromatogr. A 1044 (2004) 23–52.
[27] X.C. Lin, W.C. Zeng, X.C. Wang, Z.H. Xie, J. Sep.Sci. 32 (2009) 2767–2775.
[28] N. Ishizuka, H. Kobayashi, H. Minakuchi, K. Nakanishi, K. Hirao, K. Hosoya, T. Ikegami, N. Tanaka, J. Chromatogr. A 960 (2002) 85–96.
[29] O. Nunez, T. Ikegami, W. Kajiwara, K. Miyamoto, K. Horie, N. Tanaka, J. Chromatogr. A 1156 (2007) 35–44.
[30] J.D. Hayes, A. Malik, Anal. Chem. 72 (2000) 4090–4099.
[31] L.J. Yan, Q.H. Zhang, H. Zhang, L.Y. Zhang, T. Li, Y.Q. Feng, L.H. Zhang, W.B. Zhang, Y.K. Zhang, J. Chromatogr. A 1046 (2004) 255–261.
[32] J.F. Ma, Z. Liang, X.Q. Qiao, Q.L. Deng, D.Y. Tao, L.H. Zhang, Y.K. Zhang, Anal. Chem. 80 (2008) 2949–2956.
[33] J.F. Ma, J.X. Liu, L.L. Sun, L. Gao, Z. Liang, L.H. Zhang, Y.K. Zhang, Anal. Chem. 81 (2009) 6534–6540.
[34] L.J. Yan, Q.H. Zhang, W.B. Zhang, Y.Q. Feng, L.H. Zhang, T. Li, Y.K. Zhang, Electrophoresis 26 (2005) 2935–2941.
[35] L.J. Yan, Q.H. Zhang, Y.Q. Feng, W.B. Zhang, T. Li, L.H. Zhang, Y.K. Zhang, J. Chromatogr. A 1121 (2006) 92–98.
[36] B.H. Li, B.J. Tian, Appl. Mech. Mater. 130-134 (2012) 410–413.
[37] M. Grün, A.A. Kurganov, S. Schacht, F. Schüth, K.K. Unger, J. Chromatogr. A 740 (1996) 1–9.
[38] M. Raimondo, G. Perez, M. Sinibaldi, A. DeStefanis, A.A.G. Tomlinson, Chem. Commun. 15 (1997) 1343–1344.
[39] Y.G. Wang, F.Y. Zhang, Y.Q. Wang, J.W. Ren, C.L. Li, X.H. Liu, Y. Guo, Y.L. Guo, G.Z. Lu, Mater. Chem. Phys. 115 (2009) 649–655.